

Control of the dynamics of coupled atomic-molecular Bose-Einstein condensates: Modified Gross-Pitaevskii approach

Moumita Gupta* and Krishna Rai Dastidar†

Department of Spectroscopy, Indian Association for the Cultivation of Science, Kolkata 700032, India

(Received 5 May 2009; published 20 October 2009)

We study the dynamics of the atomic and molecular Bose-Einstein condensates (BECs) of ^{87}Rb in a spherically symmetric trap coupled by stimulated Raman photoassociation process. Considering the higher order nonlinearity in the atom-atom interaction we analyze the dynamics of the system using coupled modified Gross-Pitaevskii (MGP) equations and compare it with mean-field coupled Gross-Pitaevskii (GP) dynamics. Considerable differences in the dynamics are obtained in these two approaches at large scattering length, i.e., for large values of peak-gas parameter $x_{pk} \geq 10^{-3}$. We show how the dynamics of the coupled system is affected when the atom-molecule and molecule-molecule interactions are considered together with the atom-atom interaction and also when the strengths of these three interactions are increased. The effect of detuning on the efficiency of conversion of atomic fractions into molecules is demonstrated and the feasibility of maximum molecular BEC formation by varying the Raman detuning parameter at different values of time is explored. Thus by varying the Raman detuning and the scattering length for atom-atom interaction one can control the dynamics of the coupled atomic-molecular BEC system. We have also solved coupled Gross-Pitaevskii equations for atomic to molecular condensate formation through magnetic Feshbach resonance in a BEC of ^{85}Rb . We found similar features for oscillations between atomic and molecular condensates noted in previous theoretical study and obtained fairly good agreement with the evolution of total atomic condensate observed experimentally.

DOI: 10.1103/PhysRevA.80.043618

PACS number(s): 03.67.Mn, 05.30.Jp, 03.65.Ge

I. INTRODUCTION

The experimental success in realizing a Bose-Einstein condensate (BEC) in dilute atomic gases [1] caused a lot of experimental and theoretical activities in this field. After the observation of such atomic condensates, formation of molecular condensate gives a new dimension in the study of ultracold atomic physics. Ultracold diatomic molecules can be created starting from an ultracold atomic gas of bosons or fermions [2–5]. In order to get a signature of molecular BEC several groups have been working on magnetoassociation (Feshbach resonance) [5,6] of cold atoms to molecules. Magnetic Feshbach resonance technique is not the only possible method which can be used to form coupled atomic and molecular condensates; the production of molecular BEC can also be achieved via Raman photoassociation of atoms in a condensate. We here discuss the case of a dilute atomic BEC coupled to a molecular Bose gas by coherent Raman transitions, which has now become a matter of theoretical and experimental interest. This process of Raman photoassociation to form molecules first suggested theoretically [7–9] and further investigations on the dynamics of this coupled atomic-molecular BECs are also made [10–13]. In this case pair of atoms from the continuum state of the ground electronic potential are coupled to an excited bound molecular state by a laser field. The excited molecules are then coupled to a bound molecular state of lower energy in the ground potential by a different laser field. Experimental formation of

molecular BEC via Raman photoassociation has also been achieved [2]. Theoretically using mean-field Gross-Pitaevskii (GP) approach it is predicted that the coupled atomic and molecular system leads to a new type of “superchemistry” in which collective oscillations between the atomic and molecular condensates can occur [10–12]. It was shown [10] that Raman-transition-induced atom-molecule conversion leads to the periodic process of binding of two atoms into a molecule and vice versa and in this study the rate of these transformations is determined by the density of original atoms neglecting atom-molecule and molecule-molecule scatterings.

In the majority of theoretical studies on coupled-system dynamics the atomic scattering length has been kept fixed [10,11,13]. However the experiments on cold ^{85}Rb [14], ^{87}Rb [15], ^{133}Cs [16], ^{39}K [17], and ^7Li [18] condensates have demonstrated the variation of atomic scattering length over a wide range by using magnetic-field-induced Feshbach resonance. Though magnetic Feshbach resonances are widely used to arbitrarily tune the atom-atom interactions, alternative coupling scheme for Feshbach resonance with optical field has also been realized experimentally. Recently Theis *et al.* [19] demonstrated how the atomic scattering length a in a BEC of ^{87}Rb can change from $10a_0$ to $190a_0$ ($1 a_0=0.0529$ nm) by using one photon optical Feshbach resonance. An optical tuning of the scattering length of atoms in ^{87}Rb condensate (between $50a_0$ and $140a_0$) based on coherent free-bound Raman transitions is demonstrated by Thalhammer *et al.* [20]. Earlier for large values of scattering length, i.e., for large values of peak-gas parameter $x_{pk} \geq 10^{-3}$ ($x_{pk}=n_{pk}a^3$, where n_{pk} is the peak density of the system and a is s -wave scattering length), both the ground state

*mou_mita_81@yahoo.co.in

†krishna_raidastidar@yahoo.co.in

properties and the collective excitation frequencies of a single atomic BEC were studied by using modified Gross-Pitaevskii (MGP) theory considering higher order nonlinearity in atom-atom collision [21–25]. Previously we have shown analytically using higher order iterations in modified Thomas-Fermi model that both the ground state properties and the collective excitation frequencies are affected in presence of strong higher order nonlinearity [23,24].

The atom to molecule conversion in an atomic BEC occurs through magnetic or optical Feshbach resonance and the atom-atom scattering length may become very large near the resonance. Therefore study on the atom-molecule conversion dynamics through Feshbach resonance demands consideration of higher order nonlinearity over the mean-field GP approach. In the present work our aim is to explore the dynamics of coupled atomic and molecular BECs in the regime of high peak-gas parameter (i.e., large scattering length) by considering higher order nonlinearity for optical Feshbach resonance (Raman photoassociation). We have studied here the effect of large values of atomic *s*-wave scattering length on the dynamics of the coupled atomic-molecular BECs by considering atom-molecule and molecule-molecule interactions in addition to atom-atom interaction. We have assumed that atom-molecule and molecule-molecule scattering strengths are the same as atom-atom scattering strength [26]. Thus all the interspecies scattering strengths are increased by increasing atomic scattering length. We here uncover the change in the dynamics of the coupled atomic and molecular BECs considering the higher order nonlinear term which is described by MGP theory. The periodicity, i.e., frequency of oscillations between atomic and molecular condensates, decreases and also the densities of atoms and molecules drop at the center of the trap when higher order nonlinearity is included. Further investigations about the effect of Raman detuning on the conversion efficiency (from atoms to molecules) are also made during the evolution of the coupled system considering both GP and MGP approaches. Our study reveals that the variation in the Raman detuning and the atomic scattering length can control the depletion of atomic condensate leading to the production of molecular condensate which depends on the evolution time of the system.

Although the main aim of this paper is to show how the molecular conversion efficiency and its dynamics for ^{87}Rb condensate are affected in presence of higher order nonlinearity for different values of Raman detuning, we have also explored the dynamics of atom-molecule coherence in ^{85}Rb condensate near magnetic Feshbach resonance and compared our results with the experimental findings. In an experiment performed at JILA [5] atom-molecule coherence was observed in a BEC of ^{85}Rb atoms. The observations of this JILA experiment were described by resonant effective field theory [27] of dilute atomic gases. In this paper we have solved the coupled Gross-Pitaevskii equations to study the evolution of atomic and molecular BECs of ^{85}Rb considering magnetic Feshbach resonance and found that the oscillation between these two condensates is out of phase as obtained in case of Raman photoassociation for ^{87}Rb . Previously this feature was obtained in a parametric calculation for magnetic Feshbach resonance [28]. We have compared our theoretical results for the oscillation of atomic condensate of ^{85}Rb (in

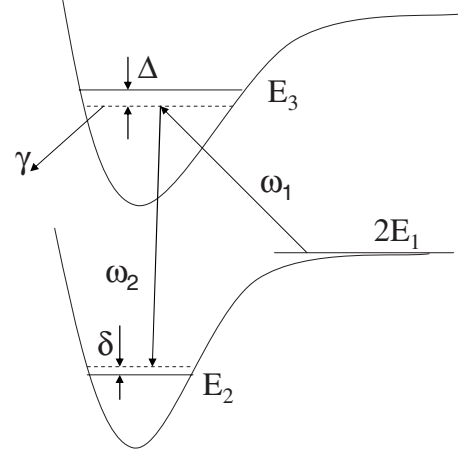


FIG. 1. Diagrammatic representation of Raman photoassociation.

presence of magnetic Feshbach resonance) with those observed in JILA experiment [5] and obtained a fairly good agreement between theoretical and experimental results for atomic population. The oscillation of molecule formation with time has also been compared with the results derived from this experiment.

The paper is organized as follows. In Sec. II A we describe the theory of coherently interacting atomic and molecular condensates coupled via stimulated Raman transitions in modified GP approach. Section II B describes the numerical method for solving the time-dependent coupled GP and MGP equations. Sections III A–III D give the results for the dynamics of the coupled system and its dependence on the different coupling strengths, higher order nonlinear term in the atom-atom collision, and the Raman detuning in ^{87}Rb condensate. In Sec. III E we have shown the results for evolution of coherence between atomic and molecular condensates of ^{85}Rb obtained by solving the coupled GP equations for magnetic Feshbach resonance and compared our results with the experimentally observed oscillation of total atomic condensate of ^{85}Rb [5]. Finally we conclude our paper in Sec. IV.

II. THEORY

A. Model

Our model is a two-color Raman photoassociation shown schematically in Fig. 1. Two atoms with total energy $2E_1$ collide to form a molecule of energy E_2 via an excited molecular state with energy E_3 . The process of stimulated Raman coupling induced by two laser fields of frequencies ω_1 and ω_2 is resonant when Raman detuning $\delta = (2E_1 - E_2)/\hbar - (\omega_2 - \omega_1)$ becomes zero. At resonance, the number of molecules formed from an atomic BEC increases considerably. In Fig. 1, one photon detuning $\Delta = (E_3 - 2E_1)/\hbar - \omega_1$ and γ is the rate of spontaneous emission from excited state. Representing atomic and molecular boson field operators by $\hat{\Psi}_a$ and $\hat{\Psi}_m$ the Hamiltonian describing the system can be written as

$$\hat{H} = \int d\vec{r} \left[\hat{\Psi}_a^\dagger \left\{ -\frac{\hbar^2}{2m} \nabla^2 + U_a(\vec{r}) + \frac{\lambda_a}{2} \hat{\Psi}_a^\dagger \hat{\Psi}_a \right\} \hat{\Psi}_a \right. \\ \left. + \hat{\Psi}_m^\dagger \left\{ -\frac{\hbar^2}{4m} \nabla^2 + \epsilon + U_m(\vec{r}) + \frac{\lambda_m}{2} \hat{\Psi}_m^\dagger \hat{\Psi}_m \right\} \hat{\Psi}_m \right. \\ \left. + \lambda_{am} \hat{\Psi}_a^\dagger \hat{\Psi}_a \hat{\Psi}_m^\dagger \hat{\Psi}_m + \frac{\chi}{2} \{ \hat{\Psi}_m^\dagger \hat{\Psi}_a \hat{\Psi}_a^\dagger \hat{\Psi}_m + \hat{\Psi}_m \hat{\Psi}_a^\dagger \hat{\Psi}_a^\dagger \} \right], \quad (1)$$

where m is the atomic mass and λ_a , λ_m , and λ_{am} are the atom-atom, molecule-molecule, and atom-molecule interaction strengths, respectively. The parameter χ describes the conversions of atoms into molecules due to stimulated Raman transitions. ϵ is a parameter to characterize Raman detuning for a two photon resonance so that $\epsilon = -\hbar\delta$. This detuning parameter ϵ can be varied either by varying one photon detuning Δ or by changing the laser frequency ω_2 . $U_a(\vec{r})$ and $U_m(\vec{r})$ are the external trap potentials for atoms and molecules.

From the above Hamiltonian GP-like equations can be obtained for the atomic and molecular mean-field operators. The operator $\hat{\Psi}$ is replaced by the classical field $\psi = \langle \hat{\Psi} \rangle$. By considering the molecular spontaneous emission, the induced decay from atomic excited state, and the light shift the GP-like equations of motion for the coupled condensate system corresponding to the Hamiltonian [Eq. (1)] become

$$i\hbar \frac{\partial \psi_a}{\partial t} = \left[-\frac{\hbar^2 \nabla^2}{2m} + U_a(\vec{r}) + \lambda_a |\psi_a|^2 + \lambda_{am} |\psi_m|^2 \right] \psi_a + \chi \psi_m \psi_a^* \\ - i\hbar \alpha \psi_a - \hbar \beta_1 \psi_a - i\hbar \Gamma_1 |\psi_a|^2 \psi_a \quad (2a)$$

and

$$i\hbar \frac{\partial \psi_m}{\partial t} = \left[-\frac{\hbar^2 \nabla^2}{4m} + U_m(\vec{r}) + \epsilon + \lambda_m |\psi_m|^2 + \lambda_{am} |\psi_a|^2 \right] \psi_m \\ + \frac{\chi}{2} \psi_a^2 - i\hbar \Gamma_2 \psi_m - \hbar \beta_2 \psi_m. \quad (2b)$$

Within Bogoliubov mean-field theory [29] atom-atom interaction strength $\lambda_a = 4\pi\hbar^2 a/m$, where a is the s -wave scattering length for atom-atom interaction. We assume here for

simplicity $\lambda_m = \lambda_{am} = \lambda_a$ [26]. For atomic condensates with large values of gas-parameter MGP theory (which includes Lee-Huang-Yang (LHY) term [30] in the interatomic interaction energy) significantly modifies the ground state and excitation frequencies of the system [23–25]. Here we have considered higher order nonlinearity (LHY term) in atom-atom interaction [23–25,30] only and hence Eq. (2a) is written as

$$i\hbar \frac{\partial \psi_a}{\partial t} = \left[-\frac{\hbar^2 \nabla^2}{2m} + U_a(\vec{r}) + \lambda_a \left(1 + \frac{32a^{3/2}}{3\pi^{1/2}} |\psi_a| \right) |\psi_a|^2 \right. \\ \left. + \lambda_{am} |\psi_m|^2 \right] \psi_a + \chi \psi_m \psi_a^* - i\hbar \alpha \psi_a - \hbar \beta_1 \psi_a \\ - i\hbar \Gamma_1 |\psi_a|^2 \psi_a \quad (3)$$

whereas Eq. (2b) remains unchanged in MGP approximation. Here $\Gamma_{1,2}$ and α are the induced decay rates and $i\beta_{1,2}\psi_{a,m}$ are the light shift terms as defined in Ref. [10]. The rate of spontaneous emission from excited state γ is included in $\Gamma_{1,2}$ as given in Eq. (8) in Ref. [10]. Solution of these two dynamical equations [Eqs. (2a) and (2b)] for atomic and molecular wave functions gives dynamics of the coupled system in GP approach and the dynamics of the coupled condensates in the MGP approach will be obtained by solving Eqs. (3) and (2b).

It is to be mentioned here that the coupled equations for magnetic Feshbach resonance can be obtained by putting $\Gamma_1 = \Gamma_2 = \beta_1 = \beta_2 = 0$ in Eqs. (2a), (2b), and (3).

B. Numerical approach

To study the dynamical properties of the coupled atomic and molecular BECs, the coupled GP equations [Eqs. (2a) and (2b)] and the coupled MGP equations [Eqs. (3) and (2b)] have been solved numerically. We consider spherically symmetric case. The trap potentials are given by $U_a(r) = \frac{1}{2} m \omega^2 r^2$ and $U_m(r) = m \omega^2 r^2$, where ω is the angular frequency and r is the radial distance. The wave function can be written as $\psi_a(r, t) = \phi_a(r, t)/r$ and $\psi_m(r, t) = \phi_m(r, t)/r$. After a transformation of variables to dimensionless quantities defined by $r = x a_{HO}$ and $t = \tau/\omega$, $a_{HO} = \sqrt{\hbar/(m\omega)}$, the coupled MGP equations [Eqs. (3) and (2b)] become

$$i \frac{\partial \phi_a}{\partial \tau} = -\frac{1}{2} \frac{d^2 \phi_a}{dx^2} + \left[\frac{1}{2} x^2 + \lambda_{a1} \left(1 + \frac{32a^{3/2}}{3\pi^{1/2}} |\phi_a| \right) \frac{|\phi_a|^2}{x^2} + \lambda_{am1} \frac{|\phi_m|^2}{x^2} - i\alpha_1 - \beta_{11} - i\Gamma_{11} \frac{|\phi_a|^2}{x^2} \right] \phi_a + \frac{\chi_1 \phi_m \phi_a^*}{x}, \quad (4)$$

$$i \frac{\partial \phi_m}{\partial \tau} = -\frac{1}{4} \frac{d^2 \phi_m}{dx^2} + \left[x^2 + \epsilon_1 + \lambda_{m1} \frac{|\phi_m|^2}{x^2} + \lambda_{am1} \frac{|\phi_a|^2}{x^2} - \beta_{21} - i\Gamma_{21} \right] \phi_m + \frac{\chi_1 \phi_m \phi_a^*}{2x}, \quad (5)$$

where $\lambda_{a1} = \lambda_a / (a_{HO}^2 \hbar \omega)$, $\lambda_{m1} = \lambda_m / (a_{HO}^2 \hbar \omega)$, $\lambda_{am1} = \lambda_{am} / (a_{HO}^2 \hbar \omega)$, $\chi_1 = \chi / (a_{HO} \hbar \omega)$, $\epsilon_1 = \epsilon / (\hbar \omega)$, $\alpha_1 = \alpha / \omega$, $\beta_{11} = \beta_1 / \omega$, $\beta_{21} = \beta_2 / \omega$, $\Gamma_{11} = \Gamma_1 / (\omega a_{HO}^2)$, and $\Gamma_{21} = \Gamma_2 / \omega$. It can be noted here that by neglecting the LHY term, i.e., the

second term in the first parenthesis on the right side of Eq. (4), it reduces to the atomic equation in the coupled GP approach and Eqs. (4) and (5) give the coupled GP equations in the transformed variables x and τ . It is assumed that at

$t=0$ the total number of atoms is N and no molecule is present in the system.

To solve Eqs. (4) and (5) the proper boundary conditions at $x=0$ and ∞ are necessary. For a confined condensate as

$$\begin{aligned} i \frac{\phi_{a,j}^{k+1} - \phi_{a,j}^k}{\Delta t} = & -\frac{1}{4h^2} [\{\phi_{a,j+1}^{k+1} - 2\phi_{a,j}^{k+1} + \phi_{a,j-1}^{k+1}\} + \{\phi_{a,j+1}^k - 2\phi_{a,j}^k + \phi_{a,j-1}^k\}] \\ & + \left[\frac{1}{2}x_j^2 + \lambda_{a1} \left(1 + \frac{32a^{3/2}|\phi_{a,j}^k|}{3\pi^{1/2}} \right) \frac{|\phi_{a,j}^k|^2}{x_j^2} + \lambda_{am1} \frac{|\phi_{m,j}^k|^2}{x_j^2} - i\alpha_1 - \beta_{11} - i\Gamma_{11} \frac{|\phi_{a,j}^k|^2}{x_j^2} \right] \frac{(\phi_{a,j}^{k+1} + \phi_{a,j}^k)}{2} + \alpha_1 \frac{\phi_{m,j}^k (\phi_{a,j}^k)^*}{x_j}, \end{aligned} \quad (6)$$

$$\begin{aligned} i \frac{\phi_{m,j}^{k+1} - \phi_{m,j}^k}{\Delta t} = & -\frac{1}{8h^2} [\{\phi_{m,j+1}^{k+1} - 2\phi_{m,j}^{k+1} + \phi_{m,j-1}^{k+1}\} + \{\phi_{m,j+1}^k - 2\phi_{m,j}^k + \phi_{m,j-1}^k\}] \\ & + \left[x_j^2 + \epsilon_1 + \lambda_{m1} \frac{|\phi_{m,j}^k|^2}{x_j^2} + \lambda_{am1} \frac{|\phi_{a,j}^k|^2}{x_j^2} - \beta_{21} - i\Gamma_{21} \right] \frac{(\phi_{m,j}^{k+1} + \phi_{m,j}^k)}{2} + \frac{\alpha_1 (\phi_{a,j}^k)^2}{2} x_j, \end{aligned} \quad (7)$$

where the discretized wave functions $\phi_{a,j}^k = \phi_a(x_j, \tau_k)$ and $\phi_{m,j}^k = \phi_m(x_j, \tau_k)$ refer to a fixed $x_j = jh$ ($j=1, 2, \dots, J_{\max}$) and $\tau_k = k\Delta t$. Considering that the wave functions $\phi_{a,j}$ and $\phi_{m,j}$ are known at time τ_k , Eqs. (6) and (7) involve the unknowns which are $\phi_{a,j+1}^{k+1}$, $\phi_{a,j}^{k+1}$, $\phi_{a,j-1}^{k+1}$, $\phi_{m,j+1}^{k+1}$, $\phi_{m,j}^{k+1}$, and $\phi_{m,j-1}^{k+1}$ at time τ_{k+1} . Equations (6) and (7) represent a tridiagonal set for $j=2$ to $J_{\max}-1$ for $\phi_{a,j}$ and $\phi_{m,j}$, which are solved with the known values of the wave functions at the end points ($\phi_{a,1}^{k+1}$, $\phi_{a,J_{\max}}^{k+1}$, $\phi_{m,1}^{k+1}$, and $\phi_{m,J_{\max}}^{k+1}$) provided by the boundary conditions (at $x=0$ and ∞) mentioned above. The tridiagonal set of Eqs. (6) and (7) is solved by Gauss elimination and back substitution method [32] using space step $h=0.001$ and time step $\Delta t=0.0001$. However a general tridiagonal matrix can also be diagonalized analytically [33,34]. In our calculations the maximum radial distance is taken to be $x_{\max}=15$ and the time evolution is studied up to $t=1$ ms. To check the accuracy of our numerical solutions we have repeated the numerical process with half of the value of both space (h) and time step (Δt) and calculate the percentage change in $N_a = \int d\vec{r} |\psi_a(\vec{r}, t)|^2$. Keeping h fixed if Δt is halved ($=0.00005$) then the percentage change in N_a is in between 0.001% and 0.3% at the positions of maxima and in between 0.1% and 0.5% at the positions of minima with increase in time. Similarly making space step h halved ($=0.0005$) and keeping Δt constant ($=0.0001$) the change in N_a is in between 0.02% and 0.1% at the positions of maxima and in between 0.03% and 0.2% at the positions of minima.

The iteration in time is started with the normalized solution of the time-independent modified Gross-Pitaevskii equation for a spherically trapped atomic condensate which is obtained by using steepest descent method [24,35]. Similarly to get the solutions for the coupled Gross-Pitaevskii equations the iteration in time should be started with the normalized solution of the time-independent uncoupled GP equation for a trapped atomic condensate [22].

$x \rightarrow \infty$, $|\phi(x, t)| \sim \exp(-x^2/4)$, and from the regularity criterion at $x=0$, $\phi=0$. Next we use the Crank-Nicholson scheme to discretize Eqs. (4) and (5) by using a space step h and time step Δt [31],

III. RESULTS AND DISCUSSIONS

The results obtained by solving the coupled GP and MGP equations for atomic and molecular condensates of ^{87}Rb have been presented here. In this calculation the values of the parameters are chosen as $\chi=\hbar \times 7.6 \times 10^{-7} \text{ m}^{3/2} \text{ s}^{-1}$, $\Gamma_1 = 1.629 \times 10^{-23} \text{ m}^3 \text{ s}^{-1}$, $\Gamma_2 = 304.4 \text{ s}^{-1}$, $\beta_1 = 2.108 \times 10^7 \text{ s}^{-1}$, $\beta_2 = 3.344 \times 10^6 \text{ s}^{-1}$, $\alpha = 134.06 \text{ s}^{-1}$, trap frequency $\omega/2\pi = 100 \text{ Hz}$, and initial number of atoms $N=5 \times 10^5$ as used in Ref. [10]. In Ref. [10] molecule-molecule (λ_m) and atom-molecule (λ_{am}) collisional interactions are neglected. Here we have considered these interactions and have assumed that $\lambda_{am} = \lambda_m = \lambda_a = 4\pi\hbar^2 a/m$ [26].

A. Effect of including molecule-molecule and atom-molecule scatterings

Figures 2 and 3 present time evolution of the atomic and molecular density profiles in GP-like approach for the detuning parameter $\delta_1 = -(\delta + \beta_2 - 2\beta_1) = 2.8 \times 10^4 \text{ s}^{-1}$ [10] and $a=5.4 \text{ nm}$ [10,36]. In Fig. 2 atom-molecule (λ_{am}) and molecule-molecule (λ_m) scattering strengths are neglected as shown in [10], whereas in Fig. 3, λ_{am} and λ_m are nonzero and equal to λ_a . The change in the dynamics of the coupled system is dramatic when the nonzero λ_{am} and λ_m are included, which is evident from Figs. 2 and 3. By comparing these two figures it is found that atomic and molecular condensates oscillate faster and the density of molecules drops by $\approx 25\%$ (at the center of the trap) due to the inclusion of molecule-molecule and atom-molecule scatterings. It can be shown that by choosing atom-molecule and molecule-molecule interactions different from atom-atom interaction [2], results will be modified differently. It is to be mentioned here that the effect of atom-molecule and molecule-molecule interactions on the dynamics will be prominent when these two interactions dominate over the parameters χ and ϵ .

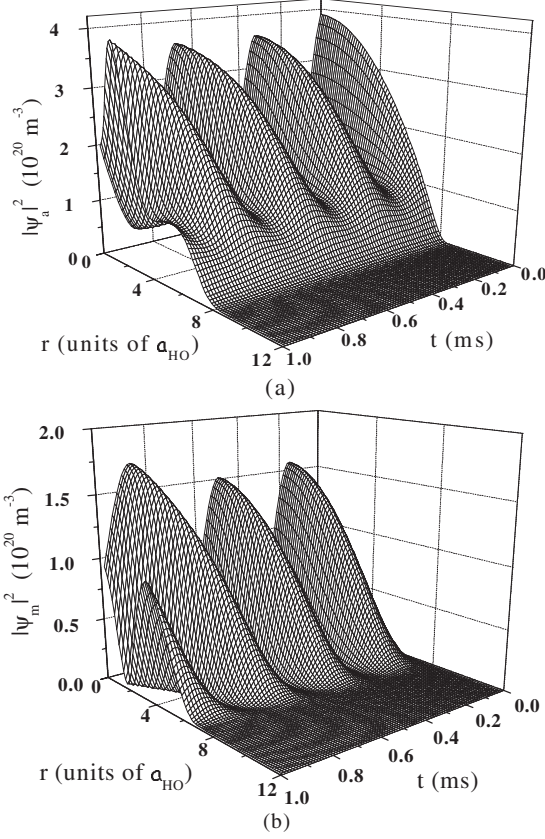


FIG. 2. Atomic (a) and molecular (b) densities $|\psi_{a,m}(r,t)|^2$ in GP approach as a function of time and radial distance for $N=5\times 10^5$, $a=5.4$ nm, and $\delta_1=2.8\times 10^4 \text{ s}^{-1}$. $\lambda_m=\lambda_{am}=0$ (λ_m and λ_{am} are the coupling strengths for molecule-molecule and atom-molecule interactions, respectively).

B. Effect of increasing the scattering length

In this work we have studied the effect of increasing atom-atom scattering length (a) on the atom-molecule coherence. Previously the effect of changes in atom-molecule interaction from attractive to repulsive with a fixed value of Raman detuning has been shown to affect the periodicity and conversion efficiency of the coupled system [12].

By optically induced Feshbach resonance using one photon scheme the atomic scattering length a in a BEC of ^{87}Rb can be tuned over a range from 0.5 to 10 nm [19]. It has also been shown that by using an optical Feshbach resonance with two photon Raman transition, atomic scattering length of ^{87}Rb BEC can be varied from 2.6 to 7.4 nm [20]. Applying a magnetic field Volz *et al.* demonstrated the variation of s -wave scattering length of ^{87}Rb over a wide range (up to ~ 35 nm) in the vicinity of a Feshbach resonance around 1007 G [15].

In this study we have considered three values of a : 5.4, 17, and 30 nm. Results for $a=5.4$ nm have been presented in Figs. 2 and 3. It has been shown here that when atomic scattering length is increased, the contribution from higher order nonlinearity (LHY term) and the strength of atom-atom interaction increase. Since we have considered $\lambda_{am}=\lambda_m=\lambda_a$, the atom-molecule and molecule-molecule interaction strengths also increase. In this section we have shown the

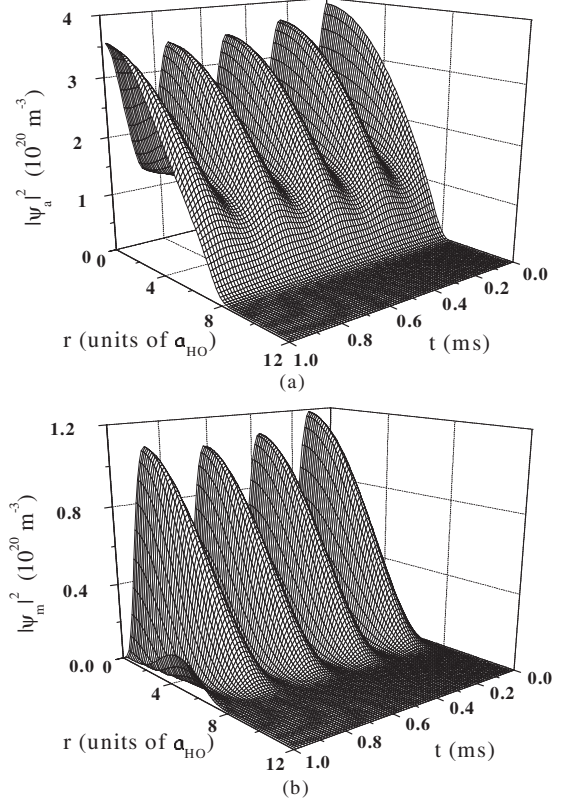


FIG. 3. Atomic (a) and molecular (b) densities $|\psi_{a,m}(r,t)|^2$ in GP approach as a function of time and radial distance for $N=5\times 10^5$, $a=5.4$ nm, and $\delta_1=2.8\times 10^4 \text{ s}^{-1}$. $\lambda_m=\lambda_{am}=\lambda_a$ (λ_a is the atom-atom interaction strength).

effect of increase in all the scattering strengths of the system by solving the GP equations. We have plotted the atomic and molecular densities as a function of time and radial distance in GP approach for $a=17$ nm (Fig. 4) with the other parameters remaining the same as in Fig. 3. Comparing Figs. 3 and 4 it is found that the increase in a leads to a decrease in the frequency of oscillations between atomic and molecular condensates and also a decrease in the density of atoms and molecules at the center of the trap by $\approx 50\%$ and $\approx 30\%$, respectively. Previously it has been shown [10] by taking different numbers of total atoms the higher density clouds oscillate faster. In this study when atom-atom scattering length is increased keeping total number of initial atoms fixed, atomic density decreases at the center and spreads out near the surface of the trap. This leads to the damped oscillations between atomic and molecular condensates. For this increased value of $a=17$ nm, if λ_{am} and λ_m are set to zero, similar effect on the dynamics (reduction in the oscillation frequency and the enhancement in the molecular density) as described in Sec. III A will be obtained.

C. Effect of higher order LHY term in atom-atom scattering strength (MGP approach)

In this section we emphasized that when scattering length a becomes large, the contribution from LHY term becomes large and affects the dynamics of the coupled system. In Fig.

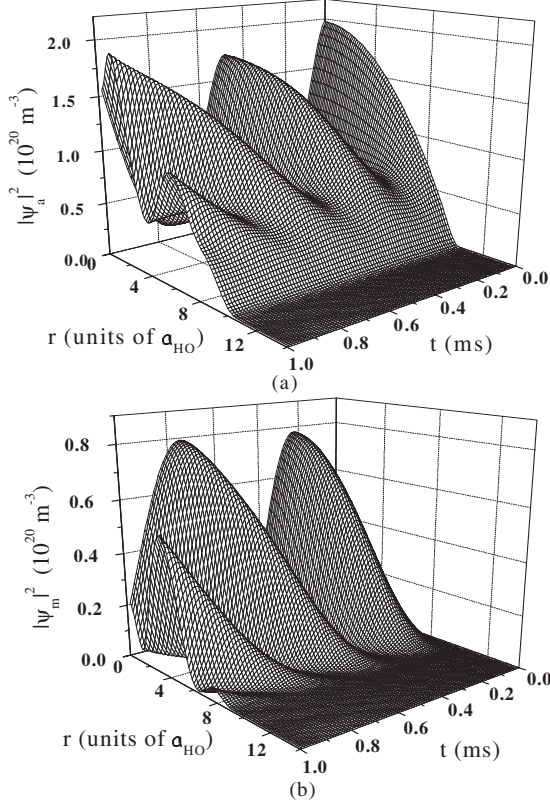


FIG. 4. Atomic (a) and molecular (b) densities $|\psi_{a,m}(r,t)|^2$ in GP approach as a function of time and radial distance for $N=5 \times 10^5$, $a=17$ nm, and $\delta_1=2.8 \times 10^4$ s $^{-1}$. $\lambda_m=\lambda_{am}=\lambda_a$.

5 we have plotted time evolution of atomic and molecular density profiles for $a=17$ nm in MGP approach (including LHY term). The effect of this term on the dynamics of the system is evident in Fig. 5, which shows that in MGP approach both the atomic and molecular condensates oscillate slowly and also the density of atoms and molecules drops at the center of the trap compared to that shown in Fig. 4. This is due to the fact that inclusion of the LHY term in the atom-atom scattering strength effectively reduces the atomic density at the center of the trap which causes further decrease in the molecular density at the center and also in the oscillation frequency. The effect of LHY term on density profile is much more prominent at higher value of scattering length, $a=30$ nm. Time evolutions of density profiles in the GP and MGP approaches are plotted in Figs. 6 and 7, respectively. The Raman detuning parameter δ_1 is chosen to be 4.6×10^4 s $^{-1}$ to get reasonably regular oscillations. In Ref. [12] atomic and molecular evolutions produced regular pattern for only first oscillation (with their best choice of detuning). But in all our results regular evolutions of densities are obtained for three to four oscillations even at large values of a by adjusting the Raman detuning appropriately. At $t=0$, peak-gas parameters (x_{pk}) of the system are 1.1×10^{-3} and 4.14×10^{-3} in GP approach and 9.41×10^{-4} and 3.36×10^{-3} in MGP approach for $a=17$ and 30 nm, respectively.

D. Effect of changing the Raman detuning

In this section we have investigated how the Raman detuning affects the conversion efficiency for molecules. By

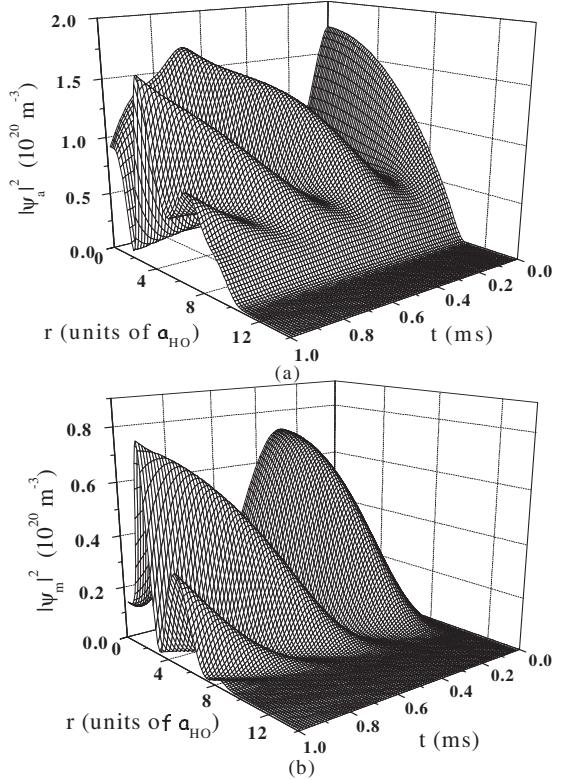


FIG. 5. Atomic (a) and molecular (b) densities $|\psi_{a,m}(r,t)|^2$ in MGP approach as a function of time and radial distance for $N=5 \times 10^5$, $a=17$ nm, and $\delta_1=2.8 \times 10^4$ s $^{-1}$. $\lambda_m=\lambda_{am}=\lambda_a$.

plotting atom number evolution with time de Oliveira and Olsen [12] showed that for a particular choice of detuning, large depletion of atomic density can be obtained from which they have inferred that the conversion efficiency will be large at that detuning. The effect of detuning on atomic and molecular populations is demonstrated here in an extensive way to show the effect of higher order nonlinearity on the atom-molecule conversion efficiency as the s -wave scattering length increases around the resonance at different evolution times. In Figs. 8 and 9, we plot the atomic and molecular populations $N_{a,m}=\int d\vec{r}|\psi_{a,m}(\vec{r},t)|^2$ as a function of δ_1 (from positive to negative values) and also as a function of time for $a=30$ nm in GP and MGP approaches, respectively. For each value of time, conversion efficiency for molecules increases significantly for a particular value of δ_1 ($=\delta_{1,max}$) and this value of $\delta_{1,max}$ changes with time. The oscillations between atomic and molecular condensates in time are also evident in these figures. The effect of the LHY term on the conversion efficiency is evident in Fig. 9 where the molecular formation (at $\delta_{1,max}$) is less than that in Fig. 8. To realize the effect of the LHY term explicitly on the conversion efficiency and also on the value of $\delta_{1,max}$, atomic and molecular populations (obtained in coupled GP and MGP approaches) are plotted for a fixed value of time when the maximum number of molecules is formed in GP approach. Figure 10 shows the results of N_a and N_m in GP and MGP approaches as a function of δ_1 for a fixed value of $t=0.24$ ms (when molecular population is maximum in GP approach) and for $a=30$ nm. It can be noted from Fig. 10 that the value of

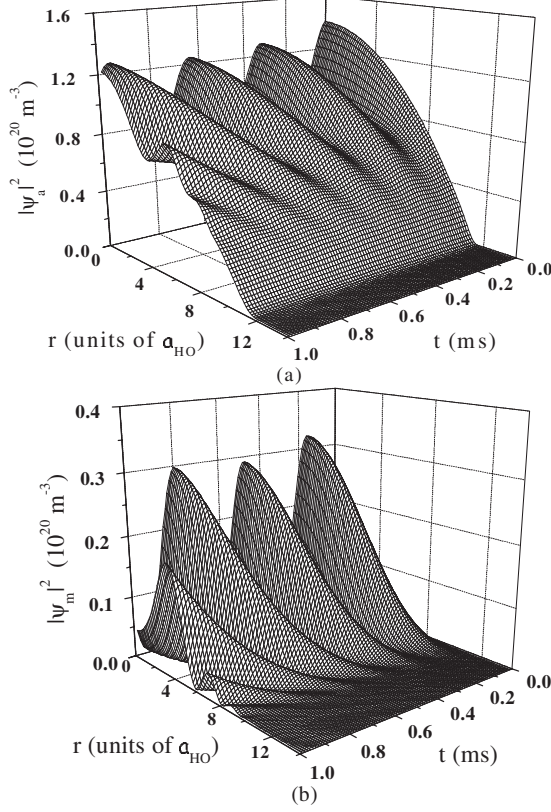


FIG. 6. Atomic (a) and molecular (b) densities $|\psi_{a,m}(r,t)|^2$ in GP approach as a function of time and radial distance for $N=5\times 10^5$, $a=30$ nm, and $\delta_1=4.6\times 10^4$ s $^{-1}$. $\lambda_m=\lambda_{am}=\lambda_a$.

$\delta_{l,\max}$ shifts toward a higher value ($=3.1\times 10^4$ s $^{-1}$) in the MGP approach in comparison to that obtained in GP approach ($=2.4\times 10^4$ s $^{-1}$). For the detuning greater than $\delta_{l,\max}$ (MGP) molecular number N_m (MGP) is higher than N_m (GP) whereas for δ_l less than $\delta_{l,\max}$ (MGP), N_m (MGP) is lower than N_m (GP). These figures clearly demonstrate how the molecular formation efficiency can be controlled by controlling the Raman detuning during the evolution of this coupled atom-molecular BEC. Similar effect of Raman detuning on the depletion of atomic condensate due to conversion to molecular condensate has been observed experimentally [2].

E. Description of the experiment on atom-molecule coherence in a BEC

In previous sections we have shown by considering higher order nonlinearity how the dynamics of atomic and molecular coherences can be controlled in ^{87}Rb by changing the strength of different interactions (atom-atom, atom-molecule, and atom-molecule) and the detuning for Raman photoassociation. In this section we have demonstrated the evolution of atom-molecular coherence in ^{85}Rb condensate in presence of magnetic Feshbach resonance for which this type of coherence has been observed experimentally [5]. We have solved the corresponding coupled GP equations for magnetic Feshbach resonance which are obtained by putting $\Gamma_1=\Gamma_2=\beta_1=\beta_2=0$ in Eqs. (2a) and (2b). We consider ^{85}Rb condens-

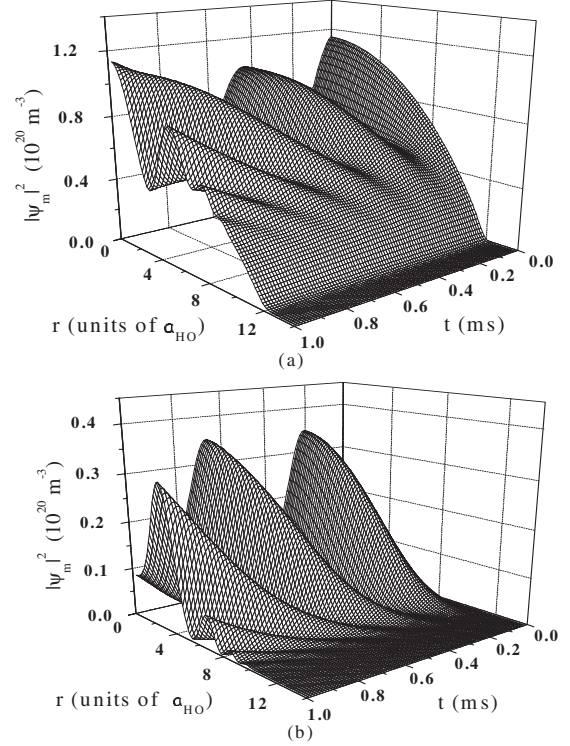


FIG. 7. Atomic (a) and molecular (b) densities $|\psi_{a,m}(r,t)|^2$ in MGP approach as a function of time and radial distance for $N=5\times 10^5$, $a=30$ nm, and $\delta_1=4.6\times 10^4$ s $^{-1}$. $\lambda_m=\lambda_{am}=\lambda_a$.

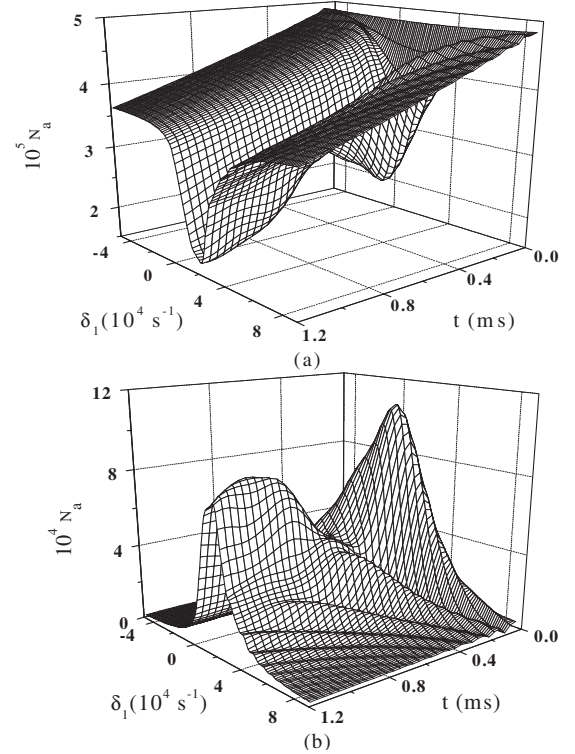


FIG. 8. Population of atoms (a) and molecules (b) $N_{a,m}=\int d\vec{r}|\psi_{a,m}(\vec{r},t)|^2$ as a function of detuning parameter δ_1 and time (t) in GP approach. $N=5\times 10^5$ and $a=30$ nm.

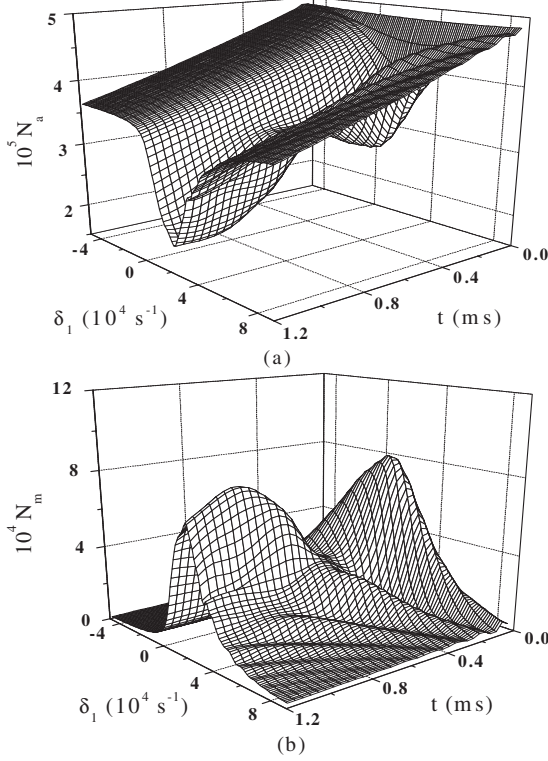


FIG. 9. Population of atoms (a) and molecules (b) $N_{a,m} = \int d\vec{r} |\psi_{a,m}(\vec{r}, t)|^2$ as a function of detuning parameter δ_1 and time (t) in MGP approach. $N=5 \times 10^5$ and $a=30$ nm.

sate in a spherically symmetric trap with frequency $\omega/2\pi = 12.69$ Hz ($=\{17.5 \times 17.2 \times 6.8\}^{1/3}$), where the experimental trap frequencies are 17.5, 17.2, and 6.8 Hz [5]. The atom-molecule coupling strength (arises due to Feshbach resonance) χ can be given in terms of resonance width (ΔB), the difference between magnetic moments of a molecule and a free atom pair ($\Delta \tilde{\mu}$), and background scattering length of atoms far from a Feshbach resonance (a_{bg}): $\chi = \sqrt{8\pi\hbar^2 a_{bg} \Delta \tilde{\mu} \Delta B / m}$ [26]. We have calculated atomic and molecular densities by considering $N=17\ 100$, $a=570a_0$,

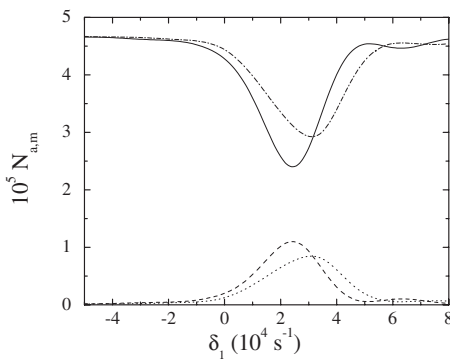


FIG. 10. Population of atoms (a) and molecules (b) $N_{a,m} = \int d\vec{r} |\psi_{a,m}(\vec{r}, t)|^2$ as a function of detuning parameter δ_1 at $t = 0.24$ ms for $a=30$ nm. Solid and dashed lines correspond to atom and molecule numbers in GP approach. Dashed-dotted and dotted lines are the atom and molecule numbers in MGP approach.

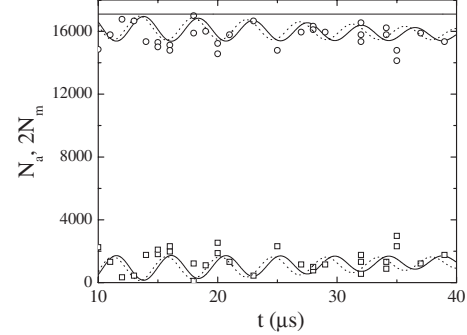


FIG. 11. Atomic (upper solid line for $\epsilon/h=195$ kHz and upper dotted line for $\epsilon/h=200$ kHz) and twice the molecular (lower solid line $\epsilon/h=195$ kHz and lower dotted line for $\epsilon/h=200$ kHz) population as a function of time. The calculation is performed for $N=17\ 100$ (indicated by the flat solid line), $a=570a_0$, $\Delta B=11$ G, and decay time=91 μ s. Open circles are the total number of observed condensate atoms taken from Fig. 6 in Ref. [5]. Open squares are the results for twice the number of molecules in the condensate (see text).

$a_{bg}=-450a_0$ (where a_0 is the Bohr radius), $\Delta B=11$ G (in [5] width of resonance $\Delta=11$ G), decay time of 91 μ s [5], and $\Delta \tilde{\mu}=-2.23\mu_B$ (where μ_B is the Bohr magneton)[27]. We have the values for ϵ/h at $B=159.84$ G by manually interpolating the solid curve of Fig. 5 in Ref. [5] (where ϵ represents the difference between the bound state energy of two atoms and the energy of a free atom pair). The error in interpolation is within 5 kHz. We have repeated the calculation with different binding energies from 195 to 200 kHz (corresponding to $B=159.84$ G) and plotted the results for the two boundary values in Fig. 11. This figure shows the population of atomic (upper solid line for $\epsilon/h=195$ kHz and upper dotted line for $\epsilon/h=200$ kHz) and twice of the molecular (lower solid line for $\epsilon/h=195$ kHz and lower dotted line for $\epsilon/h=200$ kHz) condensate as a function of time as obtained by solving coupled GP equations mentioned above. Atomic and molecular condensates show out of phase oscillations similar to that obtained in case of Raman photoassociation in ^{87}Rb . This feature is also obtained in a previous parametric calculation [28] for magnetic Feshbach resonance. In Fig. 11 the open circles are the plots of total number of experimentally observed atoms at the end of the pulse sequence taken from Fig. 6 in Ref. [5] and the open squares are the results obtained from the difference of the total number of initial condensate atoms ($N=17\ 100$) and total number of experimentally observed atoms. The open squares thus give twice the number of molecules in the condensate due to the particle conservation: $\int n(\vec{r}) d\vec{r} = \int [|\psi_a(\vec{r})|^2 + 2|\psi_m(\vec{r})|^2] d\vec{r} = N$. By comparison we find that the experimental data closely resemble our theoretical results in terms of the magnitude of atomic and molecular populations and the nature of oscillation is also very similar to that obtained from the experiment. It is to be noted here that the frequency of oscillation (shown in Fig. 11) differs from that derived from the binding energy (ϵ/h) used for this calculation by 11.1% (for $\epsilon/h=200$ kHz) to 11.3% (for $\epsilon/h=195$ kHz). Previously it was stated [28] that the molecular oscillation frequency obtained

by solving the two coupled GP equations for atomic and molecular condensates is approximately equal to the frequency corresponding to the binding energy of the molecules. It has been shown by using resonance field theory [27] that by incorporating the burst atom component and the anomalous density component the oscillation frequency corresponds to the binding energy of the molecular state. In the present study we have considered atom-molecule coupling but have not taken into account the effect of the burst atoms and the anomalous density components. The difference of the oscillation frequency from the binding energy (by 11%) may arise due to the neglect of the coupling with the burst atoms and the anomalous density components. The mean-field shift [37] is not responsible for this difference as the oscillation frequency is larger than the mean-field shift of the frequency by six orders of magnitude for the present data set. In the results given here we have considered $\lambda_{am}=\lambda_m=\lambda_a$ which means that the atom-molecule (a_{am}) and molecule-molecule (a_m) scattering lengths are the same as the atomic s -wave scattering length (a). However we have repeated the calculations with different scattering lengths for atom-molecule and molecule-molecule scatterings which are different from atom-atom scattering length [38]. It is found that the results remained unaffected even if a_{am} and a_m are increased more than by one order of magnitude. This may be due to the fact that in this system the effect of atom-molecule coupling strength (χ) and the detuning (ϵ) dominate over that of atom-molecule and molecule-molecule interactions considered here.

To describe the atom-molecule coherence for an increased value of scattering length $a=1400a_0$ as given in Fig. 4b in Ref. [5] we have considered $N=16\,500$, $\Delta B=11$ G, and $\epsilon/h=27$ kHz (obtained by interpolating the solid curve of Fig. 5 in Ref. [5]). We plot the results for atomic population in GP approach as a function of time in Fig. 12. By comparing solid line in Fig. 11 for atomic condensate with that in Fig. 12 it is found that with increase in the scattering length oscillation frequency decreases as obtained in case of Raman photoassociation in ^{87}Rb . It is to be noted that similar oscillation has been observed in remnant atoms (see Fig. 4b in Ref. [5]). It is found that the effect of higher order nonlinear interaction (LHY term) is negligible on these results because

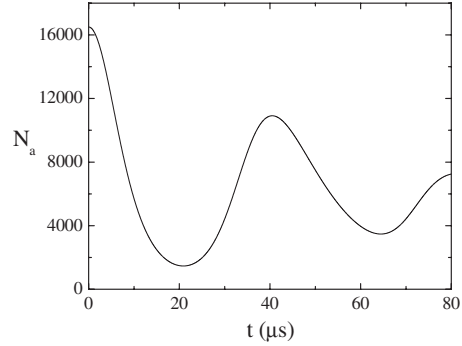


FIG. 12. Atomic population as a function of time. The calculation is performed for $N=16\,500$, $a=1400a_0$, $\Delta B=11$ G, decay time=82 μs , and $\epsilon/h=27$ kHz.

the peak-gas parameter at $t=0$ is small in both the cases (8.9×10^{-5} and 7.6×10^{-4} for Figs. 11 and 12, respectively).

IV. CONCLUSIONS

In conclusion, our investigation reveals that provided the peak-gas parameter that characterizes the scattering length of the atom-atom interaction is reasonably large ($\geq 10^{-3}$) the MGP approach (including the LHY term in the atom-atom interaction) exhibits a different dynamical behavior of the coupled atomic and molecular condensates from the mean-field GP dynamics for Raman photoassociation in ^{87}Rb condensate. The differences in dynamics are obtained in terms of oscillation frequencies and also spatial density profiles of the condensates in these two approaches. The inclusion of atom-molecule and molecule-molecule collisional strength changes the dynamics of the coupled system. We also point out that a high conversion efficiency can be reached if the Raman detuning is properly adjusted at different times. It has also been shown that the nature of oscillation of atomic and molecular condensates with time for magnetic Feshbach resonance in ^{85}Rb is similar to that obtained in case of Raman photoassociation in ^{87}Rb . The theoretical results for ^{85}Rb are compared with experimental results and found to exhibit fairly good agreement between theory and experiment.

-
- [1] M. H. Anderson *et al.*, Science **269**, 198 (1995); K. B. Davis, M. O. Mewes, M. R. Andrews, N. J. van Druten, D. S. Durfee, D. M. Kurn, and W. Ketterle, Phys. Rev. Lett. **75**, 3969 (1995); D. J. Han, R. H. Wynar, P. Courteille, and D. J. Heinzen, Phys. Rev. A **57**, R4114 (1998).
 - [2] R. Wynar, R. S. Freeland, D. J. Han, C. Ryu, and D. J. Heinzen, Science **287**, 1016 (2000).
 - [3] J. M. Gerton, D. Strekalov, I. Prodan, and R. G. Hulet, Nature (London) **408**, 692 (2000).
 - [4] S. Jochim *et al.*, Science **302**, 2101 (2003).
 - [5] E. A. Donley, N. R. Claussen, S. T. Thompson, and C. E. Wieman, Nature (London) **417**, 529 (2002).
 - [6] S. Durr, T. Volz, A. Marte, and G. Rempe, Phys. Rev. Lett. **92**, 020406 (2004).
 - [7] J. Javanainen and M. Mackie, Phys. Rev. A **58**, R789 (1998).
 - [8] J. Javanainen and M. Mackie, Phys. Rev. A **59**, R3186 (1999).
 - [9] P. D. Drummond, K. V. Kheruntsyan, and H. He, Phys. Rev. Lett. **81**, 3055 (1998).
 - [10] D. J. Heinzen, R. Wynar, P. D. Drummond, and K. V. Kheruntsyan, Phys. Rev. Lett. **84**, 5029 (2000).
 - [11] J. J. Hope and M. K. Olsen, Phys. Rev. Lett. **86**, 3220 (2001).
 - [12] F. Dimer de Oliveira and M. K. Olsen, Opt. Commun. **234**, 235 (2004).
 - [13] P. D. Drummond, K. V. Kheruntsyan, D. J. Heinzen, and R. H.

- Wynar, Phys. Rev. A **65**, 063619 (2002).
- [14] S. L. Cornish, N. R. Claussen, J. L. Roberts, E. A. Cornell, and C. E. Wieman, Phys. Rev. Lett. **85**, 1795 (2000).
- [15] T. Volz, S. Durr, S. Ernst, A. Marte, and G. Rempe, Phys. Rev. A **68**, 010702(R) (2003).
- [16] T. Weber *et al.*, Science **299**, 232 (2003).
- [17] G. Roati, M. Zaccanti, C. D'Errico, J. Catani, M. Modugno, A. Simoni, M. Inguscio, and G. Modugno, Phys. Rev. Lett. **99**, 010403 (2007).
- [18] S. E. Pollack, D. Dries, M. Junker, Y. P. Chen, T. A. Corcovilos, and R. G. Hulet, Phys. Rev. Lett. **102**, 090402 (2009).
- [19] M. Theis, G. Thalhammer, K. Winkler, M. Hellwig, G. Ruff, R. Grimm, and J. H. Denschlag, Phys. Rev. Lett. **93**, 123001 (2004).
- [20] G. Thalhammer, M. Theis, K. Winkler, R. Grimm, and J. H. Denschlag, Phys. Rev. A **71**, 033403 (2005).
- [21] A. Fabrocini and A. Polls, Phys. Rev. A **64**, 063610 (2001).
- [22] A. Fabrocini and A. Polls, Phys. Rev. A **60**, 2319 (1999).
- [23] M. Gupta and K. R. Dastidar, J. Phys.: Conf. Ser. **80**, 012038 (2007).
- [24] M. Gupta and K. R. Dastidar, J. Phys. B **41**, 195302 (2008).
- [25] A. Banerjee and M. P. Singh, Phys. Rev. A **66**, 043609 (2002).
- [26] B. Oles and K. Sacha, J. Phys. B **40**, 1103 (2007).
- [27] S. J. J. M. F. Kokkelmans and M. J. Holland, Phys. Rev. Lett. **89**, 180401 (2002).
- [28] E. Timmermans, P. Tommasini, R. Cote, M. Hussein, and A. Kerman, Phys. Rev. Lett. **83**, 2691 (1999).
- [29] N. N. Bogoliubov, J. Phys. (Moscow) **11**, 23 (1947).
- [30] T. D. Lee, K. Huang, and C. N. Yang, Phys. Rev. **106**, 1135 (1957).
- [31] S. K. Adhikari, Phys. Rev. E **62**, 2937 (2000).
- [32] W. H. Press, W. H. Flannery, S. A. Teukolsky, and W. T. Vetterling, *Numerical Recipes: The Art of Scientific Computing* Cambridge (University Press, Cambridge, 1986).
- [33] R. Usmani, Linear Algebr. Appl. **212-213**, 413 (1994).
- [34] R. Usmani, Comput. Math. Appl. **27**, 59 (1994).
- [35] K. T. R. Davies, H. Flocard, S. Krieger, and M. S. Weiss, Nucl. Phys. A **342**, 111 (1980).
- [36] J. M. Vogels, C. C. Tsai, R. S. Freeland, S. J. J. M. F. Kokkelmans, B. J. Verhaar, and D. J. Heinzen, Phys. Rev. A **56**, R1067 (1997).
- [37] D. D. Yavuz, Opt. Commun. **234**, 253 (2004).
- [38] M. W. J. Romans, R. A. Duine, S. Sachdev, and H. T. C. Stoof, Phys. Rev. Lett. **93**, 020405 (2004).